Effect of Viscosity on Long-Range Polymer Chain Dynamics in Solution Studied with a Fluorescence Blob Model

Mark Ingratta and Jean Duhamel*

Institute for Polymer Research, Department of Chemistry, University of Waterloo, 200 University Avenue West, Waterloo, ON N2L 3G1, Canada

Received August 30, 2008; Revised Manuscript Received December 17, 2008

ABSTRACT: Fluorescence dynamic quenching experiments were conducted on three series of pyrene-labeled polystyrenes in nine organic solvents to evaluate the effect that viscosity has on their long-range polymer chain dynamics (LRPCD). Two series of polystyrenes were randomly labeled with the chromophore pyrene by either a short and rigid amide linker for the CoA-PS series or a long and flexible ether linker for the CoE-PS series. The third series was obtained by end-labeling five monodisperse polystyrenes with pyrene. The monomer and excimer fluorescence decays of all pyrene-labeled polymers were acquired and analyzed with the fluorescence blob model (FBM) for the randomly labeled polymers and the Birks' scheme for the end-labeled polymers. The FBM analysis yielded the rate of excimer formation inside a blob, k_{blob}, and the size of a blob, N_{blob}. Birks' scheme analysis yielded the rate of end-to-end cyclization, k_{cy}, for a polystyrene chain length equal to N. After normalization, the products $k_{blob} \times N_{blob}$ for the randomly labeled polystyrenes and $k_{cy} \times N$ for the end-labeled polystyrenes were found to yield identical trends, confirming that any pyrene-labeled polystyrene construct reports the same information on the LRPCD of the polystyrene backbone. The products $k_{blob} \times N_{blob}$ and $k_{cy} \times N$ increased linearly with the inverse of viscosity, η^{-1}, for $\eta < 1$ mPa·s as expected for a diffusion-controlled process. However, the trends obtained with $k_{blob} \times N_{blob}$ and $k_{cy} \times N$ did not pass through the origin when $\eta^{-1} \rightarrow 0$, suggesting that excimer formation is more efficient than expected in high-viscosity solvents. N_{blob} was found to decrease with increasing viscosity. k_{blob} did not change much with viscosity in all but the most viscous solvent. The product $\eta \times k_{blob}$ was found to scale as $(N_{blob})^{-1.73}$, where the exponent of −1.73 agrees with that expected from Flory's theoretical predictions.

Introduction

Traditionally, fluorescence dynamic quenching (FDQ) experiments have been and continue to be instrumental in studying long-range polymer chain dynamics (LRPCD) in solution.[1−5] In these experiments, a chromophore (C) and its quencher (Q) are covalently attached onto a polymer. Upon absorption of a photon, the excited C (C*) can relax by either emitting a photon or being quenched by a diffusion-controlled encounter with Q. Since C and Q are covalently attached onto the chain, their encounter reflects the motions of the two monomers bearing C and Q and, thus, the LRPCD of the polymer of interest. Furthermore, fluorescence is sufficiently sensitive for FDQ experiments to be conducted at polymer concentrations so low that only intramolecular quenching events can be detected. The rate constant $\langle k_Q \rangle$ at which C* is being quenched intramolecularly by Q can be measured directly and quantitatively from the analysis of the fluorescence decays of C*. It is interesting that although the quenching of C* by Q is a bimolecular process, $\langle k_Q \rangle$ obtained from FDQ experiments conducted on labeled polymers is a pseudo-unimolecular rate constant.[3,6,7] Indeed, $\langle k_Q \rangle$ is the product of the bimolecular rate constant k_Q times the local quencher concentration $[Q]_{loc}$ inside the polymer coil. Since $[Q]_{loc}$ cannot be measured independently, all FDQ experiments conducted on labeled polymers report the product $\langle k_Q \rangle = k_Q \times [Q]_{loc}$. Since k_Q describes the collisions taking place between C* and Q, it is theoretically expected to depend on the inverse of the viscosity, η^{-1}, and numerous experimental studies on end-labeled oligomethylenes,[8,9] short end-labeled polymers,[6,10] randomly labeled polymers,[7] and short end-labeled peptides[11−13] have showed that within experimental error $\langle k_Q \rangle$ increases linearly with η^{-1}.

By and large, the bulk of FDQ studies aiming at determining $\langle k_Q \rangle$ uses the chromophore pyrene for both C and Q as the excited pyrene can undergo self-quenching by forming an excimer upon an encounter with a ground-state pyrene.[4,5] To this end, pyrene has been attached at the end of small oligomethylene chains,[9,14−22] short monodisperse polymers,[4,6,10,23−31] or dendrimers[32,33] and randomly along longer polymers.[5,7,34−42] As predicted by theory,[1−3] FDQ experiments conducted on end-labeled chains yield a single $\langle k_Q \rangle$ value, an important simplification when compared to studies dealing with randomly labeled polymers which yield a distribution of $\langle k_Q \rangle$ values.[5,34] The simpler analysis associated with the fluorescence data obtained with end-labeled polymers has led to their overwhelming use in the literature with[4,6,10,23−31] or without pyrene.[11−13,43−53] Experiments aiming at probing the effect of viscosity on LRPCD monitor the kinetics of excimer formation for pyrene end-labeled chains by either using solvents having different viscosity[7,10] or changing the temperature of the solvent.[25,28−31]

In this article, pyrene-labeled polymers are used to investigate the effect that the local pyrene concentration, $[Py]_{loc}$, has on $\langle k_Q \rangle$ by changing the solvent viscosity. As the solvent viscosity increases, excimer formation occurs only between those pyrenes that are close enough to form an excimer while a pyrene remains excited. Those pyrenes that are close enough are only found in those regions of the polymer coil where $[Py]_{loc}$ is sufficiently large. Thus, $[Py]_{loc}$ is expected to increase as the solvent viscosity increases. However, the relationship between $[Py]_{loc}$ and viscosity might not be best probed with short monodisperse end-labeled polymers, since the small coil dimension of a short chain should enable an excited pyrene to probe the entire polymer coil regardless of solvent viscosity. Consequently, $[Py]_{loc}$ is not expected to change much when using the short monodisperse chains most commonly used in the literature.[4,6,10−31,44−53] The drastic reduction in $\langle k_Q \rangle$ with increasing chain length for end-labeled polymers prevents the use of long polymers for which too few end-to-end encounters occur.[4,26]

* To whom correspondence should be addressed.

10.1021/ma8019738 CCC: $40.75
Published on Web 02/03/2009

Scheme 1. Chemical Structures of CoA-PS, CoE-PS, and PS(*X*)-Py$_2$

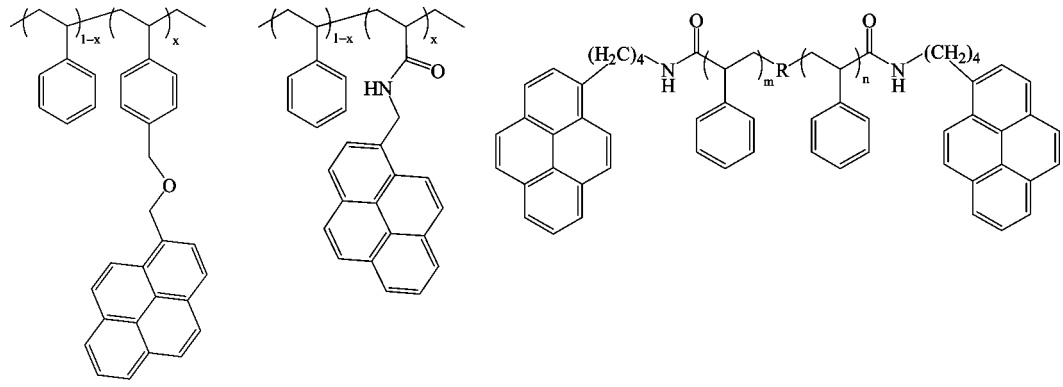

CoE–PS **CoA–PS** **PS(X)-Py$_2$**

Table 1. Pyrene Contents *x* in mol % (see Scheme 1) and λ_{Py} in μmol g^{-1}, Molecular Weights, and PDI of the CoA-PS and CoE-PS Samples

sample	*x*, mol % Py	λ_{Py}, μmol g^{-1}	M_n, kg mol^{-1}	PDI
	1.5	141	35	1.81
	1.8	169	45	1.87
CoE-PS	3.2	284	32	1.99
	4.8	412	16	1.85
	5.1	436	34	1.80
	6.4	533	46	1.65
	1.1	105	43	1.88
	2.5	230	39	2.04
CoA-PS	3.7	331	55	1.90
	5.0	437	28	1.88
	5.2	459	34	1.96
	6.4	550	39	1.91
	1.4	137	14.6	1.10
	1.6	157	12.7	1.20
PS(*X*)Py2	2.6	250	8.0	1.09
	4.6	444	4.5	1.12
	6.9	667	3.0	1.10

Table 2. Solvent Viscosities, Intrinsic Viscosities, and Solvent Qualities for PS-40K at $T = 25$ °C

solvent	η, mPa·s	$[\eta]_{40K}$, L/g	$\pm[\eta]$, L/g	solvent quality
methyl acetate	0.36	0.0159	0.0001	poor
methyl ethyl ketone (MEK)	0.41	0.0178	0.0002	poor
dichloromethane (DCM)	0.41	0.0248	0.0004	good
tetrahydrofuran (THF)	0.46	0.0246	0.0014	good
toluene	0.56	0.0259	0.0003	good
N,*N*-dimethylformamide (DMF)	0.79	0.0192	0.0003	poor
dioxane	1.18	0.0241	0.0001	good
N,*N*-dimethylacetamide (DMA)	1.92	0.0221	0.0007	mediocre
benzyl alcohol (BA)[a]	5.47			

[a] The solution in benzyl alcohol was too viscous for intrinsic viscosity measurements.

Furthermore, the inherently weak excimer emission obtained with long end-labeled polymers would be further reduced in high-viscosity solvents.[54] Considering the drastic enhancement in excimer formation observed when dealing with randomly labeled polymers,[54] we set out to monitor the effect of viscosity on $\langle k_Q \rangle$ for two series of polystyrene randomly labeled with pyrene. The fluorescence decays were analyzed with a fluorescence blob model (FBM).[5,41] The FBM is particularly well-suited for these experiments, since it yields information on the process of excimer formation taking place inside a blob which represents the volume probed by the excited pyrene during its lifetime. Excimer formation taking place inside a small or large blob yields a $\langle k_Q \rangle$ value obtained under conditions where $[Py]_{loc}$ is large or small, respectively.

To the best of our knowledge, there are only two reports in the literature where the process of excimer formation has been studied for polymers randomly labeled with pyrene in high-viscosity solvents.[7,35] In both cases, only qualitative information on the process of excimer formation was retrieved from the fluorescence intensity of the excimer over that of the monomer, the I_E/I_M ratio, obtained from the steady-state fluorescence spectra. Furthermore, the trends obtained in both manuscripts were somewhat inconsistent. In the case of poly(vinyl acetate) randomly labeled with pyrene, the I_E/I_M ratio was found to increase linearly with the inverse of viscosity ($1/\eta$) in mixtures of methanol and ethylene glycol, whereas I_E/I_M seemed to plateau for large $1/\eta$ values in mixtures of ethyl acetate and glycerol triacetate.[7] In both solvent systems, the I_E/I_M ratio tended to zero in high-viscosity solvents. When the data given for poly(methyl methacrylate) randomly labeled with pyrene in mixtures of ethyl acetate and tripropionate were used to construct a plot of the I_E/I_M ratio versus $1/\eta$, a straight line was obtained that did not pass through zero.[35]

The rather wide divergence observed in literature results based on the qualitative analysis of fluorescence spectra obtained with randomly labeled polymers in high-viscosity solvents suggests that this phenomenon is still not fully understood. The present study draws from recent advances in theoretical and analytical tools designed to study the complex photophysical processes occurring in excimer formation between pyrene pendants randomly attached onto a polymer to investigate how the rate of excimer formation changes with viscosity. This study suggests that excimer formation inside the polymer coil does not occur homogeneously, but rather inside pyrene-rich pockets which are singled out when the viscosity increases. The I_E/I_M ratio is found to decrease mostly because an increase in viscosity inhibits excimer formation and results in a larger fraction of isolated pyrene monomers. The concepts presented in this study are novel and are expected to broaden our understanding of how diffusion-controlled encounters take place between polymer segments in high-viscosity solvents.

Experimental Section

Two series of polystyrenes randomly labeled with pyrene were prepared. These polymers referred to as CoA-PS and CoE-PS were obtained from copolymerizing styrene with either 1-pyrenemethylacrylamide or 4-(1-pyrenyl)methoxymethylstyrene, respectively. Scheme 1 shows the chemical structure of the three pyrene-labeled polystyrenes, and Table 1 lists their number-average molecular weight (all substantially larger than 10 000 g·mol^{-1} for the randomly labeled polymers), polydispersity index, and pyrene content in terms of moles of pyrene per gram of polymer (λ_{Py}) or molar fraction of pyrene labeled monomer in the polymer (*x*). The short and stiff amide linker connecting pyrene to the polystyrene backbone of CoA-PS was replaced by a long and flexible ether linker for CoE-PS. One series of pyrene end-labeled monodisperse

polystyrenes was prepared by reacting 1-pyrenebutylamine with a monodisperse polystyrene terminated at both ends with a carboxylic acid functionality. The end-labeled polymers are referred to as PS(X)-Py$_2$, where X is the number-average molecular weight in kg·mol^{-1}. The synthesis and characterization of these polymers have been reported earlier.[54,55] Table 2 lists the solvents used in this study, their viscosity, and the solvent quality toward polystyrene established by intrinsic viscosity measurements.[54]

The procedure used for the acquisition of the fluorescence decays and their analysis has been reported earlier.[54] The monomer and excimer decays of CoA-PS and CoE-PS were fitted with eqs 1 and 2, respectively.

$$[\mathrm{Py}^*]_{(t)} = [\mathrm{Py}^*_{\mathrm{diff}}]_{(t=0)} \exp\left[-\left(A_2 + \frac{1}{\tau_\mathrm{M}}\right)t - A_3(1 - \exp(-A_4 t))\right] + [\mathrm{Py}^*_{\mathrm{free}}]_{(t=0)} \exp(-t/\tau_\mathrm{M}) \quad (1)$$

$$[\mathrm{E}^*] = -[\mathrm{Py}^*_{\mathrm{diff}}]_{(t=0)} \mathrm{e}^{-A_3} \sum_{i=0}^{\infty} \frac{{A_3}^i}{i!} \frac{A_2 + iA_4}{\frac{1}{\tau_\mathrm{M}} - \frac{1}{\tau_{\mathrm{E}0}} + A_2 + iA_4} \times \exp\left(-\left(\frac{1}{\tau_\mathrm{M}} + A_2 + iA_4\right)t\right) + \left([\mathrm{E}0^*]_{(t=0)} + [\mathrm{Py}^*_{\mathrm{diff}}]_{(t=0)} \mathrm{e}^{-A_3} \sum_{i=0}^{\infty} \frac{{A_3}^i}{i!} \frac{A_2 + iA_4}{\frac{1}{\tau_\mathrm{M}} - \frac{1}{\tau_{\mathrm{E}0}} + A_2 + iA_4}\right) \mathrm{e}^{-t/\tau_{\mathrm{E}0}} + [\mathrm{D}^*]_0 \mathrm{e}^{-t/\tau_\mathrm{D}} \quad (2)$$

The parameters A_2, A_3, and A_4 used in eqs 1 and 2 are described in eq 3 where $\langle n \rangle$, k_{blob}, and $k_\mathrm{e} \times$ [blob] are respectively the average number of quenchers per blob, the rate constant describing the diffusive encounter between an excited chromophore and one quencher located in the same blob, and the product of the rate constant for the exchange of quenchers between blobs and the blob concentration inside the polymer coil. Equations 1−3 have been used extensively over the past decade to study polymer chain dynamics in solution.[5]

$$A_2 = \langle n \rangle \frac{k_{\mathrm{blob}} k_\mathrm{e}[\mathrm{blob}]}{k_{\mathrm{blob}} + k_\mathrm{e}[\mathrm{blob}]} \quad A_3 = \langle n \rangle \frac{{k_{\mathrm{blob}}}^2}{(k_{\mathrm{blob}} + k_\mathrm{e}[\mathrm{blob}])^2} \quad A_4 = k_{\mathrm{blob}} + k_\mathrm{e}[\mathrm{blob}] \quad (3)$$

Four pyrene species are evoked to fit the fluorescence decays of the CoA-PS and CoE-PS series.[5] The species $\mathrm{Py}^*_{\mathrm{diff}}$ represents those pyrene monomers that form excimer by diffusive encounters inside the polymer coil. Those pyrenes that are located in pyrene-poor domains of the polymer coil and are too far to undergo any diffusive encounter with a ground-state pyrene while still being excited emit as "free" unattached pyrene labels with the natural lifetime of pyrene (τ_M) and are referred to as $\mathrm{Py}^*_{\mathrm{free}}$ in eq 1. The model also assumes that ground-state pyrene dimers are present in solution. Direct excitation of a ground-state pyrene dimer results in an excimer E0* emitting with a lifetime $\tau_{\mathrm{E}0}$ if the pyrenes are properly stacked or a long-lived dimer D* that emits with a lifetime τ_D if the pyrenes are improperly stacked.

The fluorescence intensity of the monomer and excimer decays of the PS(X)-Py$_2$ series were fitted with eqs 4 and 5, respectively.

$$I_\mathrm{M}(t) = a_{\mathrm{M}1} \exp(-t/\tau_1) + a_{\mathrm{M}2} \exp(-t/\tau_2) + a_\mathrm{M} \exp(-t/\tau_\mathrm{M}) \quad (4)$$

$$I_\mathrm{E}(t) = a_{\mathrm{E}1} \exp(-t/\tau_1) + a_{\mathrm{E}2} \exp(-t/\tau_2) \quad (5)$$

The pre-exponential factor a_M in eq 4 accounts for those polymers which are labeled at only one end and emit with the natural lifetime of the pyrene monomer (τ_M). The doubly labeled polymers exhibit a biexponential decay where the decay times τ_1 and τ_2 are the same in the monomer and excimer decays. Under conditions where strong excimer emission occurs, i.e., for short chains with degrees of polymerization smaller than 100 and fluid solvents with viscosity smaller than 1 mPa·s in the case of the PS(X)-Py$_2$ series, the ratio of the pre-exponential factors $a_{\mathrm{E}1}/a_{\mathrm{E}2}$ approaches −1.0.[54] The decay times τ_1 and τ_2 and the ratio of the pre-exponential factors $a_{\mathrm{M}1}/a_{\mathrm{M}2}$ are used to calculate the rate constants k_cy and $k_{-\mathrm{cy}}$ and the excimer lifetime τ_E according to Birks' scheme (Scheme 2).[56]

Scheme 2. Birks' Scheme for the Formation of Excimer with a Pyrene End-Labeled Monodisperse Polymer

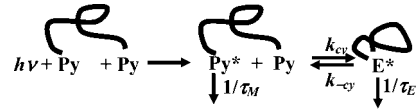

The parameters k_{blob}, $\langle n \rangle$, and k_e[blob] obtained from the analysis of the randomly labeled polystyrenes according to the FBM and k_cy, $k_{-\mathrm{cy}}$, and τ_E obtained from the Birks' scheme analysis of the end-labeled polystyrenes have been already reported in an earlier report.[54] They are listed in Tables SI.1−8 in the Supporting Information. These parameters were used earlier to demonstrate the equivalence that exists between the product $k_{\mathrm{blob}} \times \langle n \rangle$ and k_cy. Although the trends presented in the current article are based on parameters that were obtained from the same k_{blob}, $\langle n \rangle$, and k_cy values which were reported earlier,[54] all trends and their effects presented in this article have never been discussed before.

Results and Discussion

Randomly Labeled Polymers. As reported earlier,[54] the fits resulting from the global analysis of the monomer and excimer decays according to eqs 1−3 for the randomly labeled polymers CoA-PS and CoE-PS and according to eqs 4 and 5 for the end-labeled polymers PS(X)-Py$_2$ were excellent with all χ^2 being smaller than 1.30 and the residuals and autocorrelation function of the residuals being randomly distributed around zero (see Figures SI.1 and SI.2 in the Supporting Information). The parameters retrieved from these analyses are listed in Tables SI.1−8 of the Supporting Information. Excimer formation was found to occur essentially by diffusion as the presence of only low levels of ground-state (GS) pyrene dimers were found in the fluorescence decays (see the fraction of aggregated pyrenes, f_{agg}, in Tables SI.3 and SI.6 of the Supporting Information). Nevertheless, as the pyrene content of CoA-PS and CoE-PS increased, more GS pyrene dimers were found, associated with an increase in f_{agg}. To account for the presence of residual GS pyrene dimers, all trends obtained with the FBM parameters were extrapolated to zero pyrene content where no GS pyrene dimer remains. This procedure is always conducted in a FBM analysis[5,41,57,58] as it ensures that the kinetics of excimer formation approach those encountered when, first, no GS pyrene dimers are present and, second, the increased drag exerted by the covalent attachment of pyrene onto the chain becomes vanishingly small.

With a randomly labeled polymer like CoA-PS or CoE-PS, the effect that viscosity has on the distance traveled by an excited pyrene during its lifetime can be estimated from the number of monomers, N_{blob}, encompassed inside V_{blob}, which is the volume probed by the excited pyrene during its lifetime. N_{blob} is determined thanks to eq 6,[5] where $\langle n \rangle$ is the average number of pyrenes per blob, λ_{Py} is the pyrene content in mol g^{-1}, f_{Mdiff} is the molar fraction of pyrenes forming excimer by diffusion which is determined from the monomer decays as $f_{\mathrm{Mdiff}} = [\mathrm{Py}^*_{\mathrm{diff}}]_{(t=0)}/([\mathrm{Py}^*_{\mathrm{diff}}]_{(t=0)} + [\mathrm{Py}^*_{\mathrm{free}}]_{(t=0)})$, x is the molar fraction of pyrene labeled monomers in the copolymer, and M_{Py} and M_{Sty} are the molar masses of the pyrene labeled monomer (M_{Py} equals

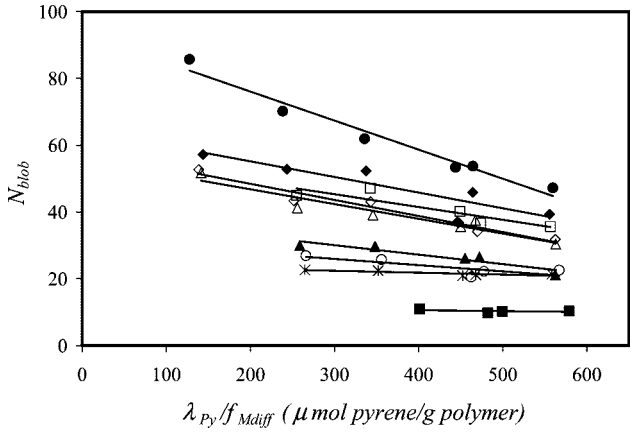

Figure 1. N_{blob} as a function of pyrene content for CoA-PS in methyl acetate (●), MEK (◆), DCM (□), THF (△), toluene (◇), DMF (▲), dioxane (○), DMA (∗), benzyl alcohol (■); [Py] = 3×10^{-6} M.

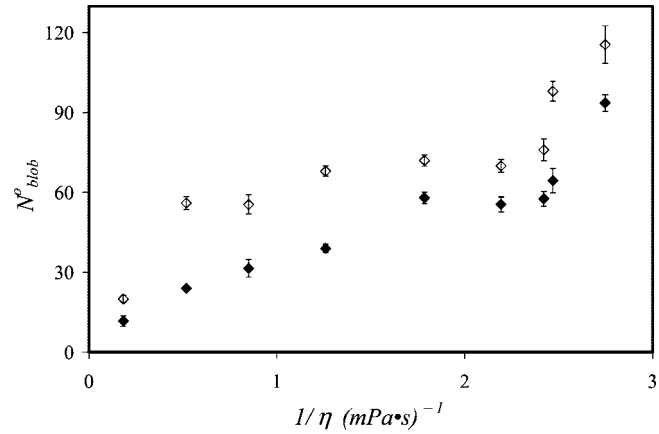

Figure 2. N°_{blob} as a function of η^{-1}. CoA-PS (◆), CoE-PS (◇); [Py] = 3×10^{-6} M.

286 and 348 g mol^{-1} for the CoA-PS and CoE-PS polymers) and styrene (104 g•mol^{-1}), respectively.

$$N_{blob} = \frac{\langle n \rangle}{\lambda_{Py}/f_{Mdiff}[M_{Py}(x) + M_{Sty}(1 - x)]} \quad (6)$$

Figure 1 shows a plot of N_{blob} versus the corrected pyrene content (λ_{Py}/f_{Mdiff}) for the CoA-PS series in nine organic solvents. The corrected pyrene content is introduced to account for those pyrene-poor regions which are generated inside the polymer coil following the random labeling of the polymer.[5,41] For pyrene contents larger than 2.5 mol %, f_{Mdiff} is close to 1.0 so that $1/f_{Mdiff}$ represents a small correction. As the viscosity increases, N_{blob} becomes smaller, as expected since a larger viscosity reduces the mobility of the excited pyrene which then probes a smaller volume. The FBM parameters are usually recovered with accuracy when f_{Mdiff} is larger than 0.85. As the viscosity increases and the excited pyrene probes a smaller volume, more pyrenes become isolated, emit a fluorescence photon before having had a chance to encounter a ground-state pyrene, and f_{Mdiff} decreases to values smaller than 0.85, even more so for the polymers having a lower pyrene content (Tables SI.1 and SI.4 of the Supporting Information). Consequently, as the viscosity increases, the results obtained with samples having a lower pyrene content are discarded which explains why much fewer N_{blob} values are being reported in Figure 1 for solvents having larger viscosities. As found in numerous other examples,[5,41,57,58] N_{blob} in a given solvent decreases linearly with increasing pyrene content due to enhanced encumbrance and drag induced by the increasing number of bulky pyrenes attached to the polymer. The N_{blob} trends shown in Figure 1 are then extrapolated to zero pyrene content to obtain an N_{blob} value representative of the naked polymer. The extrapolated N_{blob} value is referred to as N°_{blob} and is plotted as a function of the inverse of viscosity (η^{-1}) in Figure 2.

Although scattered, the trends shown in Figure 2 indicate that N°_{blob} increases with decreasing viscosity. The scatter in the trends results from the parameters, other than viscosity, that also affect the magnitude of N_{blob}. Solvent quality which leads to an expansion or contraction of the polymer coil or pyrene lifetime which controls how far diffusion will take the excited chromophore inside the polymer coil are two parameters which, beside viscosity, strongly affect N°_{blob}.[59] The combination of all these effects results in the overall trends shown in Figure 2. As also found in an earlier publication for CoA-PS and CoE-PS in THF,[55] N°_{blob} is larger for the CoE-PS than for the CoA-PS series in all organic solvents due to the longer and more flexible ether linker connecting pyrene to the CoE-PS backbone (Scheme 1).

The decrease in the number of data points available for accurate determination of N_{blob} in Figure 1 as the viscosity increases is due to the isolation of increasing numbers of pyrene moieties in the polymer coil. Indeed, f_{Mfree} in Tables SI.1 and SI.4 increases with increasing viscosity, even more so for the samples containing less pyrene. This observation implies that as the viscosity increases, the monomer emission in the fluorescence spectra increases, not because the rate of excimer formation decreases but rather because the fraction of unquenched pyrene monomer increases. This complicates the analysis of the steady-state fluorescence spectra which are used to determine the ratio I_E/I_M shown in Figure SI.3. I_E/I_M represents the ratio of the excimer fluorescence intensity (I_E) over the monomer fluorescence intensity (I_M). The ratio I_E/I_M is commonly taken as a measure of the intramolecular rate of excimer formation.[3−10,35,56] Whereas this equivalence is correct under conditions preventing the existence of isolated pyrenes (i.e., short polymer stretches separating two pyrenes, low-viscosity solvents), the data listed in Tables SI.1 and SI.4 indicate that this equivalence is not appropriate for the high-viscosity solvents ($\eta \geq 0.8$ mPa•s) used in the present study. Consequently, no attempt was made to draw conclusions from the I_E/I_M trends shown in Figure SI.3.

Whereas N°_{blob} provides information on the size of V_{blob}, information on the time scale over which chain dynamics occur inside V_{blob} is obtained with k_{blob}. As found in earlier reports,[41,55] k_{blob} was found to increase with increasing pyrene content in all solvents. The increase in k_{blob} with increasing pyrene content is internally consistent with the decrease in N_{blob} with increasing pyrene content shown in Figure 1. As the excited pyrene probes a smaller V_{blob} as implied by the smaller N_{blob} value, any excited pyrene and ground-state pyrene located inside the same blob are closer to each other, making it easier to form an excimer and resulting in a larger k_{blob} value. This observation can be rationalized with eq 7 which expresses the pseudo-unimolecular rate constant k_{blob} as the product of a diffusion-controlled bimolecular rate constant k_1^{blob} times the local concentration equivalent to one ground-state pyrene inside a blob ($1/V_{blob}$).[59] Equation 7 is the FBM equivalent of similar relationships derived for the pseudo-unimolecular rate constant of diffusional encounters taking place between two molecules inside a surfactant micelle[60] or at the end of a monodisperse polymer.[3,6,7]

$$k_{blob} = k_1^{blob}(1/V_{blob}) \quad (7)$$

Unfortunately, whereas N_{blob} decreased linearly with increasing pyrene content (Figure 1), k_{blob} did not always increase

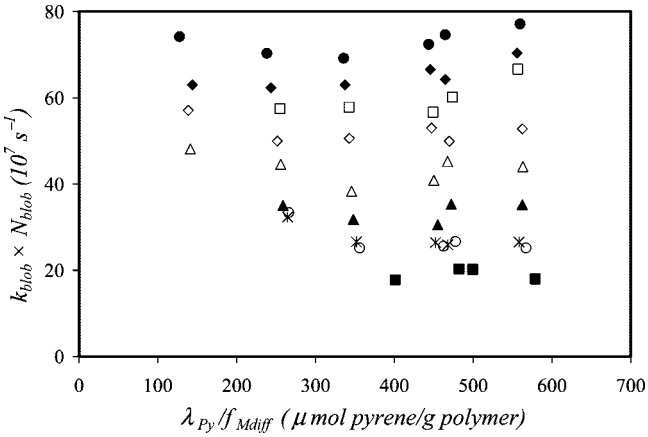

Figure 3. $k_{blob} \times N_{blob}$ as a function of pyrene content for CoA-PS in methyl acetate (●), MEK (◆), DCM (□), THF (△), toluene (◇), DMF (▲), dioxane (○), DMA (∗), and benzyl alcohol (■); [Py] = 3×10^{-6} M.

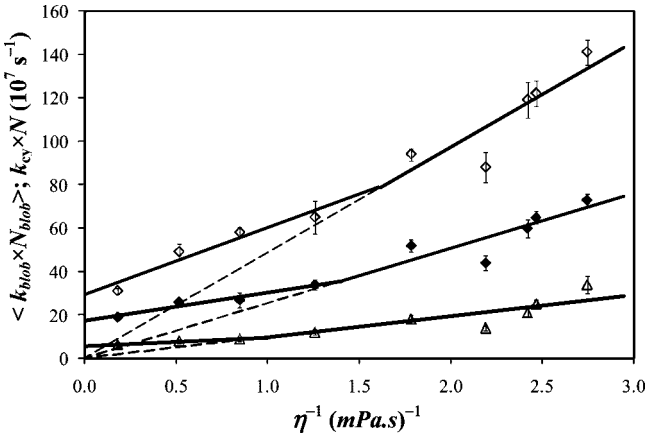

Figure 4. $\langle k_{blob} \times N_{blob} \rangle$ as a function of η^{-1} for CoA-PS (◆), CoE-PS (◇) and $k_{cy} \times N$ for PS(X)-Py_2 (△); [Py] = 3×10^{-6} M.

linearly with pyrene content, making it difficult to extrapolate the trends to zero pyrene content to find the k_{blob} value corresponding to the naked polymer. A solution to this problem was found by noting that although both N_{blob} and k_{blob} vary with pyrene content, the product $k_{blob} \times N_{blob}$ changes little with pyrene content as shown in Figure 3, where $k_{blob} \times N_{blob}$ is plotted as a function of λ_{Py}/f_{Mdiff} for the CoA-PS series in the nine organic solvents. Consequently, the trends shown in Figure 3 for the CoA-PS series were averaged over all pyrene contents to yield the quantity $\langle k_{blob} \times N_{blob} \rangle$ which was plotted as a function of η^{-1} in Figure 4.

For viscosities smaller than 1 mPa·s, $\langle k_{blob} \times N_{blob} \rangle$ is found to increase linearly with η^{-1} as expected from eq 8, which is obtained by multiplying the expression of k_{blob} in eq 7 by N_{blob}.

$$k_{blob} \times N_{blob} = k_1^{blob} \times (N_{blob}/V_{blob}) \quad (8)$$

Equation 8 is the product of the bimolecular rate constant k_1^{blob} describing diffusion-controlled encounters between pyrene pendants by the local polymer density expressed by (N_{blob}/V_{blob}). Since the local polymer density is related to the local pyrene concentration via the pyrene content of the polymer ($[Py]_{loc} = \lambda_{Py} \times M_{Sty} \times N_{blob}/V_{blob}$), $\langle k_{blob} \times N_{blob} \rangle$ is a measure of the intramolecular rate of quenching $\langle k_Q \rangle$ mentioned in the Introduction. k_1^{blob} in eqs 7 and 8 is expected to vary as η^{-1} as found in Figure 4 for the product $\langle k_{blob} \times N_{blob} \rangle$ in low-viscosity solvents.[3,6,7] Since high solvent viscosities hinder the mobility of the chain, k_1^{blob} should tend to zero for small η^{-1} values and so should $\langle k_{blob} \times N_{blob} \rangle$. Unexpectedly, this is clearly not observed for the CoA-PS and CoE-PS series in Figure 4 where extrapolation of $\langle k_{blob} \times N_{blob} \rangle$ to $\eta^{-1} \rightarrow 0$ yields a nonzero value.

The nonzero extrapolation obtained in Figure 4 implies that as the viscosity increases, the bimolecular rate constant of excimer formation k_1^{blob} or/and the local pyrene concentration $[Py]_{loc}$ is larger than expected based on the solvent viscosity alone. An increase in viscosity restricts the mobility of the chain so that excimer formation can only occur between those pyrenes that are close to each other. In the most viscous solvent, benzyl alcohol (η = 5.5 mPa·s), N_{blob} equals 12 ± 2 for CoA-PS. If the Mark−Houwink−Sakurada parameters for polystyrene in benzene at 25 °C are used to estimate the hydrodynamic volume of a 12-monomer-long chain,[61] this chain would occupy a sphere 2.9 nm^3 in volume, 18% of which would be occupied by the two pyrene moieties required to generate one excimer. This conclusion is reached by assuming that one pyrene moiety occupies a 0.26 nm^3 volume[62] and that a 12-mer polystyrene stretch adopts a spherical shape. Although this picture might be oversimplified, the argument still remains that two pyrenes located in a blob made of 12 styrene monomers are very close to each other. It implies that excimer formation occurs only in those parts of the polymer coil where $[Py]_{loc}$ is extremely large when the solvent viscosity increases beyond 1 mPa·s. It must be also noted that not only is $[Py]_{loc}$ expected to be large, but so is k_1^{blob}. Indeed, an excited pyrene confined in such a small volume with a GS pyrene would not need to undertake an extensive spatial search of a GS pyrene in its surroundings to form an excimer, as is required in lower viscosity solvents where $[Py]_{loc}$ inside the much larger blob is much smaller. Thus, the kink observed in the trends shown in Figure 4 for CoA-PS and CoE-PS is believed to result from a switch in regime where excimer formation occurs between those pyrenes that are close to each other in high-viscosity solvents and those pyrenes that are far from each other in low-viscosity solvents. However, it must be acknowledged that the above discussion based on $[Py]_{loc}$ is by no means a definite proof of the origin of this effect, but should rather be considered as a possible starting point for further investigations on this effect.

End-Labeled Polymers. In the case of randomly labeled polymers such as CoA-PS and CoE-PS, two pyrenes can be found close to each other either because (1) they are attached on two consecutive monomers along the chain or (2) coiling of the chain has brought two pyrenes attached at far flung locations along the chain in close proximity. To assess the reason behind the effect observed in Figure 4, the product $k_{cy} \times N$ was plotted for the end-labeled polymers PS(X)-Py_2 as a function of η^{-1} in Figure 4. This was done for the two following reasons. First, the observation that $N°_{blob}$ retrieved in the high-viscosity solvents yielded values smaller than or similar to the chain length of the shorter PS(X)-Py_2 samples implied that the nonzero extrapolation found in Figure 4 for the CoA-PS and CoE-PS series should also be observed with the shorter end-labeled polystyrenes, since their coil dimension should be larger than the expected size of a blob in a high-viscosity solvent. Second, in the case of the end-labeled polymers, an excimer can only be generated from the encounter between two pyrenes attached onto far-flung locations along the chain, namely the chain ends in the case of the PS(X)-Py_2 series.

The fluorescence decays of the PS(X)-Py_2 samples were acquired and analyzed with eqs 4 and 5 for the pyrene monomer and excimer, respectively. The analysis for the end-labeled polymers was found to deviate somewhat from the Birks' scheme in the higher viscosity solvents, even for the shorter PS(X)-Py_2 samples with $X \leq 8$ selected in this study. PS(X)-Py_2 samples with a larger X value do not yield enough excimer to apply the Birks' scheme analysis to the fluorescence

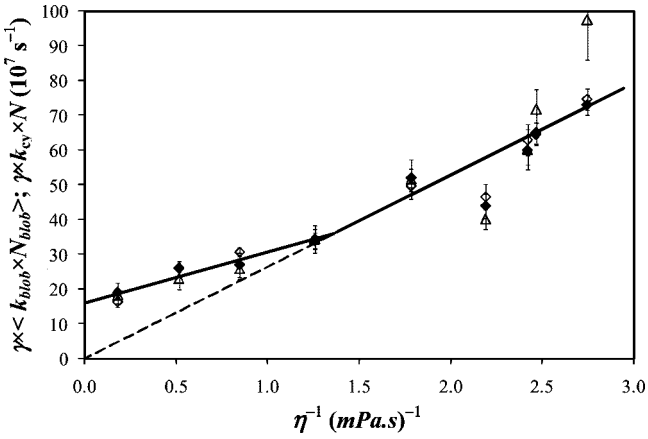

Figure 5. $\gamma \times \langle k_{blob} \times N_{blob} \rangle$ as a function of η^{-1} for CoA-PS (γ = 1.0; ◆), CoE-PS (γ = 0.5; ◇) and $\gamma \times k_{cy} \times N$ for PS(X)-Py_2 (γ = 2.9; △); [Py] = 3×10^{-6} M.

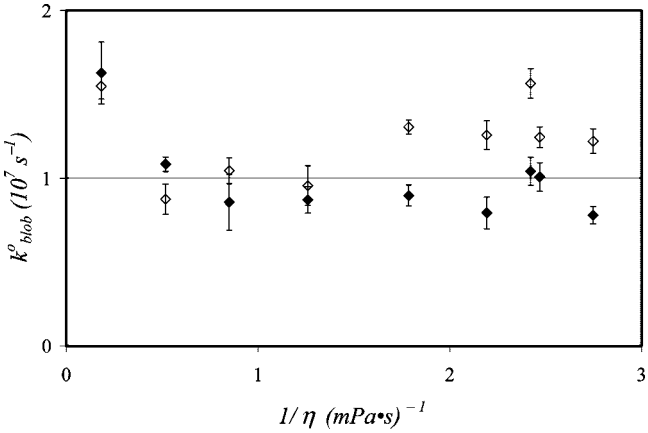

Figure 6. k^{o}_{blob} as a function of η^{-1}. CoA-PS (◆), CoE-PS (◇); PS(X)-Py_2 (△); [Py] = 3×10^{-6} M.

decays.[24,54] The ratio of the pre-exponential factors associated with the rise time and decay time obtained from the analysis of the excimer fluorescence decays, a_{E-}/a_{E+}, is commonly used to quantify the proportion of excimers that are formed via diffusion vs excimers formed via preassociated dimers.[21,28,36,37,42,57,58] An a_{E-}/a_{E+} ratio close to −1.0 indicates that all excimer formation occurs via diffusion, while a value close to zero indicates usually that excimers are formed via ground-state dimers. For the PS(X)-Py_2 samples with $X \leq 8$ in solvents with a relatively low viscosity ($\eta \leq 1.2$ mPa·s), the a_{E-}/a_{E+} ratio equals ∼−0.95, indicating that most excimer formation occurs via diffusion. However, as the polymer chain length or the solvent viscosity is increased, the ratio increases toward zero (Table SI.7) with the a_{E-}/a_{E+} ratio increasing to the more positive value of −0.92 ± 0.01 in DMA (η = 1.93 mPa·s) and further to −0.82 ± 0.04 in benzyl alcohol (η = 5.47 mPa·s). The a_{E-}/a_{E+} ratios different from −1.0 obtained in the higher viscosity solvents could reflect the presence of ground-state pyrene dimers,[21,28,36,37,42,57,58] but they are more likely due to the monomer species "leaking" into the excimer region of the fluorescence spectrum. This conclusion is reached by considering that (1) pyrene is well-soluble in organic solvents like those used in the present study, (2) the pyrene end groups of PS(X)-Py_2 are held apart from each other by the chain, and (3) excimer formation is considerably reduced in high-viscosity solvents.[7,10,54] Certainly, the dramatically weak excimer formation in DMA and benzyl alcohol results in the monomer fluorescence leaking into the fluorescence decay of the excimer. Fortunately, monomer leakage into the excimer decay affects the a_{E-}/a_{E+} ratio but not k_{cy} retrieved from the analysis of the monomer decays.

Comparison between Randomly and End-Labeled Polymers. Since k_{cy} could be obtained only with the three shorter end-labeled polymers PS(3)-Py_2, PS(4.5)-Py_2, and PS(8)-Py_2 with M_n < 10 000 g mol^{-1} for reasons which were discussed earlier (i.e., too weak excimer formation),[54] the products $k_{cy} \times N$ obtained with these three samples were averaged and plotted as a function of η^{-1} in Figure 4. The same trend found for $\langle k_{blob} \times N_{blob} \rangle$ of the CoA-PS and CoE-PS series was observed for $k_{cy} \times N$ of the PS(X)-Py_2 series. This can be seen more clearly in Figure 5 where the products $\langle k_{blob} \times N_{blob} \rangle$ for the CoA-PS and CoE-PS series and $k_{cy} \times N$ for the PS(X)-Py_2 series were multiplied by the scaling factor γ equal to 1.0, 0.5, and 2.9, respectively. The trends obtained with $\langle k_{blob} \times N_{blob} \rangle$ for CoA-PS and CoE-PS and $k_{cy} \times N$ for PS(X)-Py_2 are equivalent. This equivalence is not fortuitous. It arises first from the similarity that exists between eqs 8 and 9.

$$k_{cy} \times N = k_1^{cy} \times (N/V_{coil}) \quad (9)$$

As for k_{blob} in eq 8, k_{cy} in eq 9 is a pseudo-unimolecular rate constant which is the product of a bimolecular rate constant k_1^{cy} that describes the diffusion-controlled encounters between an excited pyrene and a ground-state pyrene both located inside the volume V_{coil} occupied by the polymer coil.[3,6,7]

As implied by the similarity of eqs 8 and 9, the products $k_{blob} \times N_{blob}$ and $k_{cy} \times N$ appear to represent the same physical phenomenon that relates the kinetics of excimer formation (k_1^{blob} and k_1^{cy}) to a polymer chain length (N_{blob} and N). The scaling factor γ accounts for differences in k_1^{blob}, k_1^{cy}, and the local polymer density N_{blob}/V_{blob} and N/V_{coil} associated with each series of pyrene-labeled polymer.[54] The similarity of the trends obtained with $k_{blob} \times N_{blob}$ and $k_{cy} \times N$ is further supported by the fact that $k_{blob} \times N_{blob}$ equals $k_{blob} \times \langle n \rangle / x$ (where x = molar fraction of labeled styrene monomer) for randomly labeled polymers containing enough pyrene so that $f_{Mdiff} \approx 1.0$, $k_{cy} \times N$ equals $2 \times k_{cy}/x$ for the end-labeled polymers, and the quantities $k_{blob} \times \langle n \rangle / x$ and k_{cy}/x have been shown to yield identical trends with viscosity after being multiplied by a constant scaling factor.[54]

The condition that f_{Mdiff} be equal to unity arises from the equivalence one would like to have between the pyrene content of the polymer given by x and the average number of pyrenes per blob given by $\langle n \rangle$. Whereas this equivalence holds at high pyrene contents, it fails at lower pyrene contents where an f_{Mdiff} value smaller than 1.0 implies that a non-negligible fraction of pyrenes are isolated monomers and excimer formation occurs in pyrene-rich pockets of the polymer coil. In this case, $\langle n \rangle$ reflects the large $[Py]_{loc}$ of the pyrene-rich pockets which is larger than expected from considering x. The heterogeneity in excimer formation at low pyrene content prevents one from using the quantity $k_{blob} \times \langle n \rangle / x$ for samples where f_{Mdiff} is substantially smaller than unity, which was consistently observed for the CoA-PS sample containing 1.1 mol % pyrene. Because the calculation of N_{blob} accounts for this heterogeneity by using the corrected pyrene content λ_{Py}/f_{Mdiff} in eq 6, the product $k_{blob} \times N_{blob}$ can be used with the 12 polymer samples in most solvents (see Figure SI.4 for example), even if f_{Mdiff} is smaller than unity although f_{Mdiff} needs to be larger than ∼0.80 to ensure that the parameters k_{blob} and $\langle n \rangle$ are retrieved with sufficient accuracy. The use of $k_{blob} \times N_{blob}$ represents thus an improvement over that of $k_{blob} \times \langle n \rangle / x$ which should prove valuable in future FBM studies.

Figures 4 and 5 indicate that both $\langle k_{blob} \times N_{blob} \rangle$ for the randomly labeled polymers and $k_{cy} \times N$ for the end-labeled polymers do not pass through the origin when $\eta^{-1} \rightarrow 0$. Since

this result is also obtained with the PS(X)-Py_2 constructs whose structure minimizes the formation of ground-state dimers, it implies that in high-viscosity solvents excimer formation for the randomly labeled polymers occurs between pyrenes that are attached onto monomers located at far-flung positions along the chain and not pyrenes that were incorporated next to each other during the random copolymerization that yielded the CoA-PS and CoE-PS samples. In other words, the trends shown in Figures 4 and 5 reflect the LRPCD of polystyrene chains.

The trends obtained in Figures 4 and 5 have been rationalized by considering the changes expected in $[Py]_{loc}$ during pyrene excimer formation as the solvent viscosity increases. It is interesting to note that nearby pyrene pairs can be selected over pyrene pairs separated by longer distances not only by adjusting the viscosity of the solution but also by reducing the lifetime of pyrene via addition of an external quencher to the solution.[58,59] Reducing the time window available for encounters due to LRPCD by either increasing the solvent viscosity or reducing the lifetime of the excited chromophore should result in the same effect, as observed in the present and earlier reports.[58,59] In fact, adjusting the viscosity of the solution or the lifetime of the chromophore to emphasize side-chain dynamics over LRPCD is a well-known practice when using fluorescence anisotropy.[63,64] It is thus satisfying that effects induced by changes in solvent viscosity or chromophore lifetime are probed in a similar fashion by both fluorescence dynamic quenching or fluorescence anisotropy experiments.

Scaling Effect between $\eta \times k^{\circ}_{blob}$ and N°_{blob}. Since k_{blob} does not always increase linearly with pyrene content, a measure of k_{blob} representative of the naked polymer (k°_{blob}) is obtained by dividing $\langle k_{blob} \times N_{blob} \rangle$ in Figure 4 by N°_{blob} given in Figure 3 (see Figure SI.4 for a more detailed description of the procedure). A plot of k°_{blob} versus the inverse of viscosity is shown in Figure 6. In most cases, k°_{blob} is slightly larger for the CoE-PS series than for the CoA-PS series. Bare benzyl alcohol, k°_{blob} does not change much with viscosity for both series, although it could be argued that k°_{blob} for the CoE-PS series exhibits a small increase with decreasing viscosity. Whatever be the case, k°_{blob} varies much less than would be expected if k°_{blob} were inversely proportional to viscosity considering that the viscosity increases more than 5-fold between methyl acetate ($\eta = 0.36$ mPa·s) and N,N-dimethylacetamide ($\eta = 1.92$ mPa·s). k°_{blob} takes an average value of 1.0 ± 0.3 and $1.2 \pm 0.2 \times 10^7$ s^{-1} for CoA-PS and CoE-PS, respectively. The steadiness of k°_{blob} with viscosity can be readily explained with eq 7. As the viscosity increases, the excited pyrene probes a smaller volume V_{blob} and encounters diffusively a ground-state pyrene with a smaller rate constant k_1^{blob} which is expected to be inversely proportional to the viscosity. Both effects appear to cancel each other, resulting in a k°_{blob} value that depends little on viscosity, as suggested in an earlier publication.[59] The substantially larger k°_{blob} value obtained in benzyl alcohol might be a result of the substantially smaller N°_{blob} value obtained in this high-viscosity solvent (Figure 3). As mentioned earlier, two pyrenes located in a small blob result in a large $[Py]_{loc}$ where excimer formation occurs more efficiently and with a larger k_1^{blob} value than in lower viscosity solvents where diffusion-controlled encounters occur over larger distances.

The data obtained with the FBM can also be used to investigate the scaling effects which are so often encountered in polymeric systems.[65] According to eq 7, $V_{blob} = k_1^{blob}/k_{blob}$ where k_1^{blob} is inversely proportional to viscosity so that V_{blob} is expected to be inversely proportional to the product $\eta \times k_{blob}$. A plot of $\ln(\eta \times k^{\circ}_{blob})$ vs $\ln(N^{\circ}_{blob})$ is shown in Figure 7. Linear trends are obtained for both the CoA-PS and CoE-PS series with slopes equal to -1.68 ± 0.02 and -1.77 ± 0.03, respectively, with an average of 1.73. This result implies that

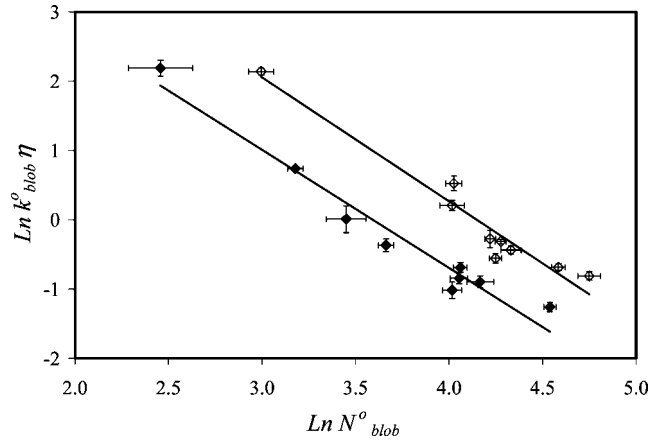

Figure 7. $\ln(k^{\circ}_{blob} \times \eta)$ as a function of $\ln(N^{\circ}_{blob})$. CoA-PS (◆), CoE-PS (◇); $[Py] = 3 \times 10^{-6}$ M.

V_{blob} scales as $N_{blob}^{1.73}$. Similar scaling laws have been observed when a series of poly(*N*,*N*-dimethylacrylamide)s randomly labeled with pyrene was studied with the FBM in acetone and DMF. In this case, V_{blob} had been found to scale as N_{blob}^{α}, where α equaled 1.4 and 1.8 in acetone and DMF, respectively.[59] The exponent of 1.73 reflects the open conformation of the polymer coil. A much larger exponent α has been found for the relationship $V_{blob} \propto N_{blob}^{\alpha}$ in the case of a pyrene-labeled poly(L-glutamic acid) which adopted a much denser α-helical conformation.[58] In the case of end-labeled monodisperse polymers, k_{cy} has been reported to scale as N^{α}, where α takes values between 1.4 and 1.7.[4,13,22,24,46,47] The equivalence observed between the end-labeled and randomly labeled polymers found for the products $k_{blob} \times N_{blob}$ and $k_{cy} \times N$ in Figure 5 seems to hold also in terms of the similar exponent α retrieved for the scaling laws that are expected between k_{blob} and N_{blob} for randomly labeled polymers and k_{cy} and N for the end-labeled monodisperse polymers.

Conclusions

Using FDQ experiments, the LRPCD of two series of polystyrene randomly labeled with pyrene (CoA-PS and CoE-PS) and one series of pyrene end-labeled polystyrene (PS(X)-Py_2) have been characterized by using either the FBM for the randomly labeled polymers or the Birks' scheme for the end-labeled polymers. The LRPCD of polystyrene was monitored in nine organic solvents with viscosities ranging from 0.34 to 5.47 mPa·s. All polymer constructs experienced slower LRPCD upon increasing the solvent viscosity as the products $k_{blob} \times N_{blob}$ and $k_{cy} \times N$ increased linearly with η^{-1} for viscosities smaller than 1 mPa·s (Figures 4 and 5). Interestingly, $k_{blob} \times N_{blob}$ and $k_{cy} \times N$ did not pass through the origin when the trends were extrapolated to $\eta^{-1} \rightarrow 0$ in Figures 4 and 5. This result suggests that excimer formation occurs at a rate faster than expected from considering viscosity alone. As importantly, the equivalence observed between the products $k_{blob} \times N_{blob}$ and $k_{cy} \times N$ in Figure 5 demonstrated that both types of polymer constructs, namely, the long polydisperse polystyrenes randomly labeled with pyrene or the short monodisperse polystyrenes end-labeled with pyrene, yield the same information on LRPCD. Beside the numerous experimental advantages associated with using randomly labeled polymers which have been reviewed earlier,[54] the FBM provides information on the volume V_{blob} probed by an excited pyrene during its lifetime in the form of N°_{blob}. N°_{blob} represents the number of monomers encompassed inside V_{blob}. As the viscosity increases, N°_{blob} decreases and tends to zero (Figure 2). Finally, the scaling laws typically encountered in polymer physics are also observed with the parameters

retrieved from a FBM analysis in the form of the relationship $\eta \times k^{\circ}_{blob} \propto (N^{\circ}_{blob})^{\alpha}$, where α was found to equal -1.68 ± 0.02 and -1.77 ± 0.03 for CoA-PS and CoE-PS, respectively.

Acknowledgment. Mark Ingratta and Jean Duhamel acknowledge financial support from an Ontario's Premier Research Excellence Award and NSERC. J.D. is indebted to the CFI funding associated with his Tier-2 CRC award.

Supporting Information Available: Figure SI.1, fits of the monomer and excimer fluorescence decays for CoE-PS in DMF; Figure SI.2, fits of the monomer and excimer fluorescence decays for CoA-PS in DMF; Figure SI.3, plot of the I_E/I_M ratio divided by the pyrene content as a function of $1/\eta$ for the three series of polystyrenes labeled with pyrene; Figure SI.4, description of the procedure used to determine k°_{blob}; Tables SI.1−8, parameters retrieved from the fit of the fluorescence decays using eqs 1−5. This material is available free of charge via the Internet at http://pubs.acs.org.

References and Notes

(1) Wilemski, G.; Fixman, M. *J. Chem. Phys.* **1974**, *60*, 866–877.
(2) Wilemski, G.; Fixman, M. *J. Chem. Phys.* **1974**, *60*, 878–890.
(3) Cuniberti, C.; Perico, A. *Prog. Polym. Sci.* **1984**, *10*, 271–316.
(4) Winnik, M. A. *Acc. Chem. Res.* **1985**, *18*, 73–79.
(5) Duhamel, J. *Acc. Chem. Res.* **2006**, *39*, 953–960.
(6) Cuniberti, C.; Perico, A. *Eur. Polym. J.* **1977**, *13*, 369–374.
(7) Cuniberti, C.; Perico, A. *Eur. Polym. J.* **1980**, *16*, 887–893.
(8) Emert, J.; Behrens, C.; Goldenberg, M. *J. Am. Chem. Soc.* **1979**, *101*, 771–772.
(9) Wang, F. W.; Lowry, R. E.; Grant, W. H. *Polymer* **1984**, *25*, 690–692.
(10) Cheung, S.-T.; Winnik, M. A.; Redpath, A. E. C. *Makromol. Chem.* **1982**, *183*, 1815–1824.
(11) Bieri, O.; Wirz, J.; Hellrung, B.; Schutkowski, M.; Drewello, M.; Kiefhaber, T. *Proc. Natl. Acad. Sci. U.S.A.* **1999**, *96*, 9597–9601.
(12) Möglich, A.; Krieger, F.; Kiefhaber, T. *J. Mol. Biol.* **2005**, *345*, 153–162.
(13) Neuweiler, H.; Löllmann, M.; Doose, S.; Sauer, M. *J. Mol. Biol.* **2007**, *365*, 856–869.
(14) Pandey, S.; Kane, M. A.; Baker, G. A.; Bright, F. V.; Fürstner, A.; Seidel, G.; Leitner, W. *J. Phys. Chem. B* **2002**, *106*, 1820–1832.
(15) Gardinier, W. E.; Kane, M. A.; Bright, F. V. *J. Phys. Chem. B* **2004**, *108*, 18520–18529.
(16) Gardinier, W. E.; Bright, F. V. *J. Phys. Chem. B* **2005**, *109*, 14824–14829.
(17) Kanaya, T.; Goshiki, K.; Yamamoto, M.; Nishijima, Y. *J. Am. Chem. Soc.* **1982**, *104*, 3580–3587.
(18) Almeida, L. M.; Vaz, W. L. C.; Zachariasse, K. A.; Madeira, V. M. C. *Biochemistry* **1982**, *21*, 5972–5977.
(19) Zachariasse, K. A.; Duveneck, G.; Busse, R. *J. Am. Chem. Soc.* **1984**, *106*, 1045–1051.
(20) Zachariasse, K. A.; Duveneck, G. *J. Am. Chem. Soc.* **1987**, *109*, 3790–3792.
(21) Reynders, P.; Kühnle, W.; Zachariasse, K. A. *J. Am. Chem. Soc.* **1990**, *112*, 3929–3939.
(22) Zachariasse, K. A.; Maçanita, A. L.; Kühnle, W. *J. Phys. Chem. B* **1999**, *103*, 9356–9365.
(23) Winnik, M. A.; Redpath, T.; Richards, D. H. *Macromolecules* **1980**, *13*, 328–335.
(24) Svirskaya, P.; Danhelka, J.; Redpath, A. E. C.; Winnik, M. A. *Polymer* **1983**, *24*, 319–322.
(25) Redpath, A. E. C.; Winnik, M. A. *J. Am. Chem. Soc.* **1982**, *104*, 5604–5607.
(26) Winnik, M. A.; Redpath, A. E. C.; Paton, K.; Danhelka, J. *Polymer* **1984**, *25*, 91–99.
(27) Xu, H.; Martinho, J. M. G.; Winnik, M. A.; Beinert, G. *Makromol. Chem.* **1989**, *190*, 1333–1343.
(28) Farinha, J. P. S.; Martinho, J. M. G.; Xu, H.; Winnik, M. A.; Quirk, R. P. *J. Polym. Sci., Part B: Polym. Phys.* **1994**, *32*, 1635–1642.
(29) Martinho, J. M. G.; Reis e Sousa, A. T.; Winnik, M. A. *Macromolecules* **1993**, *26*, 4484–4488.
(30) Reis e Sousa, A. T.; Castanheira, E. M. S.; Fedorov, A.; Martinho, J. M. G. *J. Phys. Chem. A* **1998**, *102*, 6406–6411.
(31) Farinha, J. P. S.; Piçarra, S.; Miesel, K.; Martinho, J. M. G. *J. Phys. Chem. B* **2001**, *105*, 10536–10545.
(32) Brauge, L.; Caminade, A.-M.; Majoral, J.-P.; Slomkowski, S.; Wolszczak, M. *Macromolecules* **2001**, *34*, 5599–5606.
(33) Danko, M.; Libiszowski, J.; Biela, T.; Wolszczak, M.; Duda, A. *J. Polym. Sci., Part A: Polym. Chem.* **2005**, *43*, 4586–4599.
(34) Winnik, M. A.; Egan, L. S.; Tencer, M.; Croucher, M. D. *Polymer* **1987**, *28*, 1553–1560.
(35) Wang, F. W.; Lowry, R. E. *Polymer* **1985**, *26*, 1046–1052.
(36) Seixas de Melo, J.; Costa, T.; Miguel, M. da G.; Lindman, B.; Schillen, K. *J. Phys. Chem. B* **2003**, *107*, 12605–12621.
(37) Seixas de Melo, J.; Costa, T.; Francisco, A.; Maçanita, A. L.; Gago, S.; Gonçalves, I. S. *Phys. Chem. Chem. Phys.* **2007**, *9*, 1370–1385.
(38) Picarra, S.; Relogio, P.; Afonso, C. A. M.; Martinho, J. M. G.; Farinha, J. P. S. *Macromolecules* **2003**, *36*, 8119–8129.
(39) Picarra, S.; Relogio, P.; Afonso, C. A. M.; Martinho, J. M. G.; Farinha, J. P. S. *Macromolecules* **2004**, *37*, 1670–1670.
(40) Picarra, S.; Duhamel, J.; Fedorov, A.; Martinho, J. M. G. *J. Phys. Chem. B* **2004**, *108*, 12009–12015.
(41) Mathew, H.; Siu, H.; Duhamel, J. *Macromolecules* **1999**, *32*, 7100–7108.
(42) Kanagalingam, S.; Ngan, C. F.; Duhamel, J. *Macromolecules* **2002**, *35*, 8560–8570.
(43) Horie, K.; Schnabel, W.; Mita, I.; Ushiki, H. *Macromolecules* **1981**, *14*, 1422–1428.
(44) Hagen, S. J.; Hofrichter, J.; Szabo, A.; Eaton, W. A. *Proc. Natl. Acad. Sci. U.S.A.* **1996**, *93*, 11615–11617.
(45) McGimpsey, W. G.; Chen, L.; Carraway, R.; Samaniego, W. N. *J. Phys. Chem. A* **1999**, *103*, 6082–6090.
(46) Lapidus, L. J.; Eaton, W. A.; Hofrichter, J. *Proc. Natl. Acad. Sci. U.S.A.* **2000**, *97*, 7220–7225.
(47) Krieger, F.; Fierz, B.; Bieri, O.; Drewello, M.; Kiefhaber, T. *J. Mol. Biol.* **2003**, *332*, 265–274.
(48) Fierz, B.; Satzger, H.; Root, C.; Gilch, P.; Zinth, W.; Kiefhaber, T. *Proc. Natl. Acad. Sci. U.S.A.* **2007**, *104*, 2163–2168.
(49) Fierz, B.; Kiefhaber, T. *J. Am. Chem. Soc.* **2007**, *129*, 672–679.
(50) Möglich, A.; Joder, K.; Kiefhaber, T. *Proc. Natl. Acad. Sci. U.S.A.* **2006**, *103*, 12394–12399.
(51) Hudgins, R. R.; Huang, F.; Gramlich, G.; Nau, W. M. *J. Am. Chem. Soc.* **2002**, *124*, 556–564.
(52) Huang, F.; Hudgins, R. R.; Nau, W. M. *J. Am. Chem. Soc.* **2004**, *126*, 16665–16675.
(53) Roccatano, D.; Sahoo, H.; Zacharias, M.; Nau, W. M. *J. Phys. Chem. B* **2007**, *111*, 2639–2646.
(54) Ingratta, M.; Hollinger, J.; Duhamel, J. *J. Am. Chem. Soc.* **2008**, *130*, 9420–9428.
(55) Ingratta, M.; Duhamel, J. *Macromolecules* **2007**, *40*, 6647–6657.
(56) Birks, J. B. *Photophysics of Aromatic Molecules*. Wiley: New York, 1970; p 301.
(57) Duhamel, J.; Kanagalingam, S.; O'Brien, T.; Ingratta, M. *J. Am. Chem. Soc.* **2003**, *125*, 12810–12822.
(58) Ingratta, M.; Duhamel, J. *J. Phys. Chem. B* **2008**, *112*, 9209–9218.
(59) Kanagalingam, S.; Spartalis, J.; Cao, T.-C.; Duhamel, J. *Macromolecules* **2002**, *35*, 8571–8577.
(60) Almgren, M.; Löfroth, J.-E. *J. Colloid Interface Sci.* **1981**, *81*, 486–499.
(61) Altares, T.; Wyman, D. P.; Allen, V. R. *J. Polym. Sci., Part A* **1964**, *2*, 4533–4544.
(62) Robertson, J. M.; White, J. G. *J. Chem. Soc.* **1947**, 358–68.
(63) Bentz, J. P.; Beyl, J. P.; Beinert, G.; Weill, G. *Eur. Polym. J.* **1975**, *11*, 711–718.
(64) Gorovits, B. M.; Horowitz, P. M. *J. Biol. Chem.* **1995**, *270*, 13057–13062.
(65) de Gennes, P.-G. *Scaling Concepts in Polymer Physics*; Cornell University Press: Ithaca, NY, 1979.
(66) Flory, P. J. *Principles of Polymer Chemistry*; Cornell University Press: Ithaca, NY, 1953.

MA8019738